Chapter 12

Search for Higgs Boson in Non-SUSY Models

12.1 Scalar sector of 5D Randall-Sundrum model

The Randall-Sundrum model (RS) [93, 646] has recently received much attention because it could provide a solution to the hierarchy problem [565], by means of an exponential factor in a five dimensional nonfactorisable metric. In the simplest version the RS model is based on a five dimensional universe with two four-dimensional hypersurfaces (branes), located at the boundary of the fifth coordinate. By placing all the Standard Model fields on the visible brane all the mass terms, which are of the order of the Planck mass, are rescaled by the exponential factor, to a scale of the order of a TeV. The fluctuations in the metric in the fifth dimension are described in terms of a scalar field, the radion, which in general mixes with the Higgs boson. This scalar sector of the RS model is parameterised in terms of a dimensionless Higgs boson radion mixing parameter ξ, of the Higgs boson and radion masses $\mathrm{m_h}$, m_ϕ and the vacuum expectation value of the radion field Λ_ϕ.

The phenomenology of Higgs boson and radion at LHC has been subject to several studies [647–652] concentrating mainly on Higgs and radion processes. The Higgs boson and radion detection is not guaranteed in all the parameter space region. The presence in the Higgs radion sector of trilinear terms opens the possibility of $\phi \rightarrow \mathrm{hh}$ and $\mathrm{h} \rightarrow \phi\phi$ decays. For example, for $\mathrm{m_h}$= 120 GeV/c^2, Λ_ϕ=5 TeV/c^2 and m_ϕ ∼250-350 GeV/c^2 the BR($\phi \rightarrow \mathrm{hh}$) ranges between 20 and 30%.

The CMS discovery potential is estimated for the decay of the radion in a pair of Higgs bosons, with $\gamma\gamma\mathrm{b\bar{b}}$, $\tau\tau\mathrm{b\bar{b}}$ and $\mathrm{b\bar{b}b\bar{b}}$ final states and for an integrated luminosity of 30 fb^{-1}. The study has been carried out for the radion mass of 300 GeV/c^2 and the Higgs boson mass of 125 GeV/c^2. The sensitivity was evaluated in the (ξ,Λ_ϕ) plane, with systematics uncertainties included.

A detailed description of the analysis can be found in [653]. A brief summary of the analysis and the results is presented below.

12.1.1 The $\phi \rightarrow \mathrm{hh}$ analysis with the $\gamma\gamma\mathrm{b\bar{b}}$ and $\tau\tau\mathrm{b\bar{b}}$ final states.

Signal events $\mathrm{gg} \rightarrow \phi \rightarrow \mathrm{hh}$ were generated with PYTHIA. The cross sections and branching ratios were evaluated using rescaled NLO cross sections for the SM Higgs boson and a modified HDECAY program. For the radion and a Higgs boson mass points considered ($\mathrm{m_h}$=125 GeV/c^2, m_ϕ=300 GeV/c^2) and for Λ_ϕ= 1 TeV/c^2 the maximal cross section times branching ratio is 71 fb for $\gamma\gamma\mathrm{b\bar{b}}$ final state. For the $\tau\tau\mathrm{b\bar{b}}$ final state with the topology considered in the analysis, one τ lepton decaying leptonically and the other τ lepton decaying hadronically (producing a τ jet), the maximal cross section times branching ratio is 960 fb. This maximal

cross section is reached for the radion mixing parameter $\xi = -0.35$.

For the $\gamma\gamma b\bar{b}$ final state the irreducible backgrounds $\gamma\gamma jj$ (j=u,d,s,g) (generated with COMPHEP) and the $\gamma\gamma c\bar{c}$ and $\gamma\gamma b\bar{b}$ (generated with MADGRAPH) were studied. The reducible background from γ+three jets and four-jet processes was not evaluated directly, but assumed to be the same as in for the inclusive $h \to \gamma\gamma$ analysis [19], namely 40 % of the total background after all selection. For the $\tau\tau b\bar{b}$ final state, the $t\bar{t}$, Z+jets, W+jets backgrounds (generated with PYTHIA) and the $b\bar{b}Z$ background (generated with COMPHEP) were studied.

The $\gamma\gamma b\bar{b}$ events were required to pass the Level-1 and HLT diphoton trigger. In the off-line analysis two photon candidates with $E_T^{\gamma 1,\gamma 2} > 40$, 25 GeV were required to pass tracker cuts and calorimeter isolation cuts. Events with only two calorimeter jets of E_T >30 GeV and within $|\eta|$ <2.4 were selected. At least one of these jets must be tagged as a b-jet. Finally, the diphoton mass, $M_{\gamma\gamma}$, was required to be in a window of $\pm$ 2 GeV/c^2, the dijet mass, $M_{j\bar{b}}$, in a window of $\pm$ 30 GeV/c and the diphoton-dijet mass, $M_{\gamma\gamma b\bar{b}}$, in a window $\pm$ 50 GeV/c^2 around the Higgs and Radion mass. Figure 12.1 shows the dijet (left plot) and the diphoton (right plot) mass distribution for the background (open histogram) and the signal of $\phi \to hh \to \gamma\gamma b\bar{b}$ (full, black histogram) after all selections except the mass window cuts, and for 30 fb^{-1}. The signal is shown for the maximal cross section times branching ratios point in (ξ-Λ_ϕ) plane. Figure 12.2 (left plot) shows the $M_{\gamma\gamma bj}$ distribution for the background (dashed

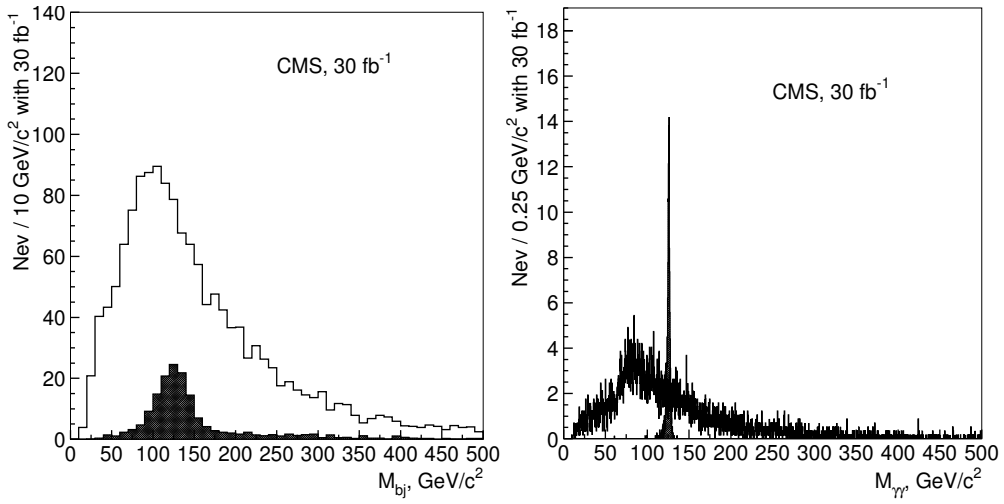

Figure 12.1: The dijet (left plot) and the diphoton (right plot) mass distribution for the background (open histogram) and the signal of $\phi \to hh \to \gamma\gamma b\bar{b}$ (full black histogram) after all selections except the mass window cuts with 30 fb^{-1}. The signal is shown for the maximal cross section times branching ratios point in (ξ-Λ_ϕ) plane.

histogram) and for the signal of $\phi \to hh \to \gamma\gamma b\bar{b}$ plus background (solid histogram) after all selections, and for 30 fb^{-1}.

The $\tau\tau b\bar{b}$ events were selected by the single electron and muon triggers and by the combined e-plus-τ-jet and the μ-plus-τ-jet triggers. In the off-line analysis a lepton and τ-jet identification was performed. The requirements on the jets were similar to the ones used in the $\gamma\gamma b\bar{b}$ analysis. In addition a cut of the transverse mass of the lepton and missing transverse momentum, $M_T^{\ell\nu}$ <35 GeV/c^2 was applied to suppress the $t\bar{t}$ and W+jets backgrounds. The diτ-lepton mass was reconstructed using the missing transverse energy as described in Sec-

tion 5.2.5. The significance of the discovery was calculated using expected number of the signal and background events after the mass window selections: $100< \mathrm{M_{bj}} <150\,\mathrm{GeV/c^2}$, $100< \mathrm{M_{\tau\tau}} <160\,\mathrm{GeV/c^2}$ and $280< \mathrm{M_{\tau\tau bj}} <330\,\mathrm{GeV/c^2}$. Figure 12.2 (right plot) shows the $\mathrm{M_{\tau\tau bj}}$ distribution for the background (full, gray histogram) and for the signal of $\phi \rightarrow \mathrm{hh} \rightarrow \tau\tau\mathrm{b\bar{b}}$ plus background (black points with the error bars) after all selections, for $30\,\mathrm{fb^{-1}}$. Fitted curves for the background and the signal plus background are superimposed.

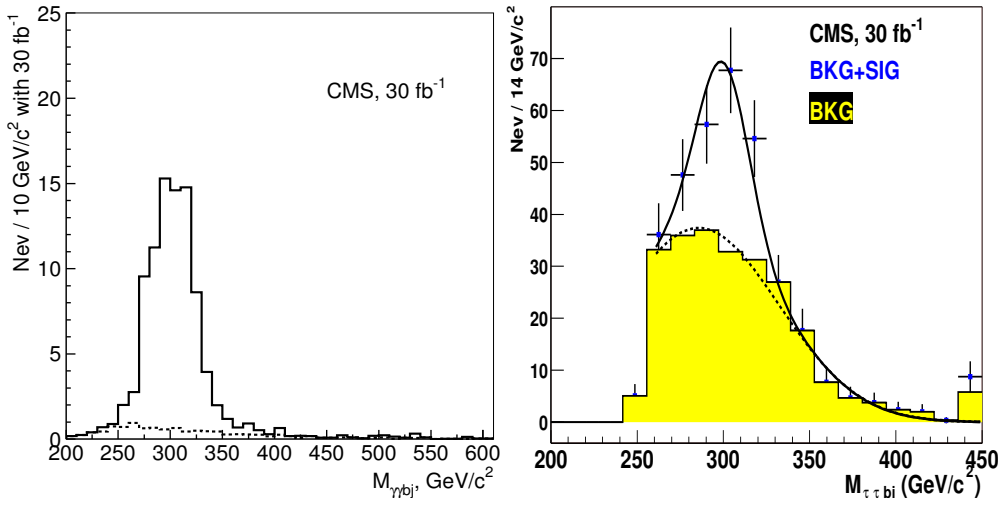

Figure 12.2: Left plot: the $\mathrm{M_{\gamma\gamma bj}}$ distribution for the background (dashed histogram) and for the signal of $\phi \rightarrow \mathrm{hh} \rightarrow \gamma\gamma\mathrm{b\bar{b}}$ plus background (solid histogram) after all selections for $30\,\mathrm{fb^{-1}}$. Right plot: the $\mathrm{M_{\tau\tau bj}}$ distribution for the background (full gray histogram) and for the signal of $\phi \rightarrow \mathrm{hh} \rightarrow \tau\tau\mathrm{b\bar{b}}$ plus background (black points with the error bars) after all selections for $30\,\mathrm{fb^{-1}}$. The fitted curves for the background and signal plus background are superimposed. On both plots the signal is shown for the maximal cross section times branching ratios point in (ξ-Λ_ϕ)

The four b-jet final state yields the highest rate for the signal. The maximal cross section times branching ratio at $\Lambda_\phi = 1\,\mathrm{TeV/c^2}$ is 10.3 pb, which results in about 3.1×10^5 signal events for $30\,\mathrm{fb^{-1}}$. The effective triggering and selection in the off-line analysis of these events is, however a big challenge due to the huge multi-jet background rate. In fact the remaining background is a few orders of magnitude larger than the signal in the relevant mass range. Techniques can be envisaged to normalise the background directly from a signal-free region and predict the number of background events in the signal region. In order to make a 3σ discovery, such extrapolation needs to be performed with a precision of about 0.1%, making four b-jet channel essentially hopeless.

The background contribution to the $\gamma\gamma\mathrm{b\bar{b}}$ final state can be determined directly from the $\gamma\gamma$-plus-two-jets data obtained after all selections, except the final mass window cuts on the $\mathrm{M_{\gamma\gamma}}$, $\mathrm{M_{j\bar{b}}}$ and $\mathrm{M_{\gamma\gamma b\bar{b}}}$. The signal-to-background ratio is always less than 10 % before the mass cuts are applied. The final cuts on the $\mathrm{M_{\gamma\gamma}}$, $\mathrm{M_{j\bar{b}}}$ and $\mathrm{M_{\gamma\gamma b\bar{b}}}$ introduce a systematic uncertainty on the number of the background events expected after these cuts. This uncertainty is determined by the following factors: the energy scale uncertainty for the photons and jets, and the theoretical uncertainty of the shape of the mass distributions due to the scale and PDF uncertainties. Figure 12.3 (left plot) shows the 5σ discovery contours for the $\phi \rightarrow \mathrm{hh} \rightarrow \gamma\gamma\mathrm{b\bar{b}}$ channel for $30\,\mathrm{fb^{-1}}$. The solid (dashed) contour shows the discovery region without (with)

the effects of the systematic uncertainties.

For the $\tau\tau b\bar{b}$ final state the background uncertainty due to the experimental selections was estimated to be between 5% and 10% [653]. Figure 12.3 (right plot) shows the 5σ discovery contours for the $\phi \rightarrow hh \rightarrow \tau\tau b\bar{b}$ channel for $30\,fb^{-1}$. The two contours corresponds to the variation of the background NLO cross sections due to the scale uncertainty. The 5% experimental systematics on the background is taken into account.

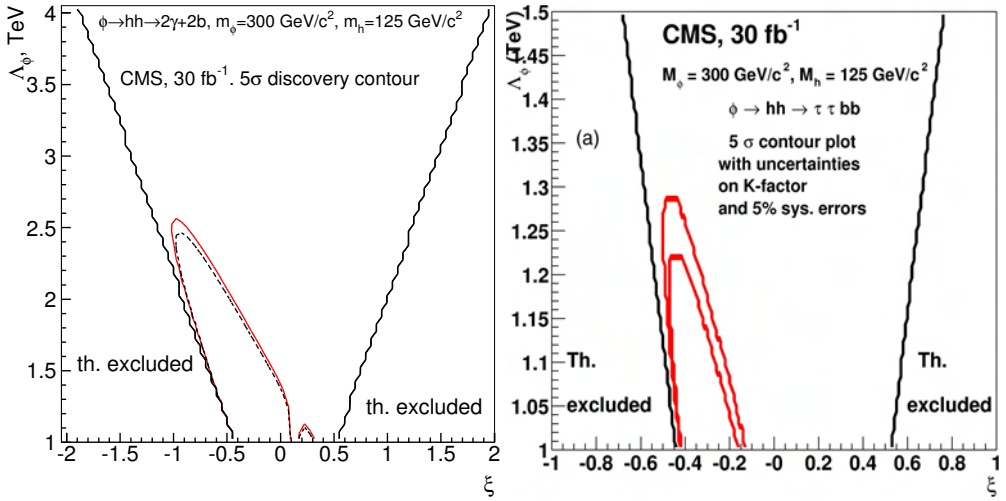

Figure 12.3: Left plot: the 5σ discovery contours for the $\phi \rightarrow hh \rightarrow \gamma\gamma b\bar{b}$ channel for $30\,fb^{-1}$. The solid (dashed) contour shows the discovery region without (with) the effects of the systematic uncertainties (find more explanations in the text). Right plot: the 5σ discovery contours for the $\phi \rightarrow hh \rightarrow \tau\tau b\bar{b}$ channel for $30\,fb^{-1}$. The two contours corresponds to the variation of the background NLO cross sections due to the scale uncertainty. The 5% experimental systematics on the background is taken into account (see text).

12.2 Doubly charged Higgs boson pair production in the Littlest Higgs model

The main motivation of the Large Hadron Collider (LHC) experiments is to reveal the secrets of electroweak symmetry breaking. If the standard model (SM) Higgs boson will be discovered, the question arises what stabilises its mass against the Planck scale quadratically divergent radiative corrections. The canonical answer to this question is supersymmetry which implies very rich phenomenology of predicted sparticles in the future collider experiments.

More recently another possibility of formulating the physics of electroweak symmetry breaking, called the little Higgs, was proposed [654–656]. In those models the SM Higgs boson is a pseudo Goldstone mode of a broken global symmetry and remains light, much lighter than the other new modes of the model which have masses of order the symmetry breaking scale $\mathcal{O}(1)$ TeV. In order to cancel one-loop quadratic divergences to the SM Higgs mass a new set of heavy gauge bosons W', Z' with the SM quantum numbers identical to W Z, and a vector like heavy quark pair T, $\bar{T}$ with charge 2/3 must be introduced. Notice that those fields are put in by hand in order to construct a model with the required properties. However, the minimal model based on the $SU(5)/SO(5)$ global symmetry, the so-called littlest Higgs

model [657], has a firm prediction from the symmetry breaking pattern alone: the existence of another $\mathcal{O}(1)$ TeV pseudo Goldstone boson Δ with the $SU(2)_L \times U(1)_Y$ quantum numbers $\Delta \sim (3, 2)$.

Interestingly, the existence of triplet Higgs Δ might also be required to generate Majorana masses to the left-handed neutrinos [658]. Non-zero neutrino masses and mixing is presently the only experimentally verified signal of new physics beyond the SM. In the triplet neutrino mass mechanism [659] the neutrino mass matrix is generated via

$$(m_\nu)_{ij} = (Y_\Delta)_{ij} v_\Delta, \tag{12.1}$$

where $(Y_\Delta)_{ij}$ are the Majorana Yukawa couplings of the triplet to the lepton generations $i, j = e, \mu, \tau$ which are described by the Lagrangian

$$L = i\bar{\ell}^c_{Li} \tau_2 Y^{ij}_\Delta (\tau \cdot \Delta) \ell_{Lj} + h.c., \tag{12.2}$$

and v_Δ is the effective vacuum expectation value of the neutral component of the triplet induced via the explicit coupling of Δ to the SM Higgs doublet H as $\mu \Delta^0 H^0 H^0$. Here μ has a dimension of mass. In the concept of seesaw $\mu \sim M_\Delta$, and the smallness of neutrino masses is attributed to the very high scale of triplet mass M_Δ via the smallness of $v_\Delta = \mu v^2 / M^2_\Delta$, where $v = 174$ GeV.

However, in the littlest Higgs model the triplet mass scale is $\mathcal{O}(1)$ TeV which alone cannot suppress v_Δ. Therefore in this model $\mu \ll M_\Delta$, which can be achieved, for example, via shining from extra dimensions as shown in ref. [660, 661] or if the triplet is related to the Dark Energy of the Universe [662]. In that case $v_\Delta \sim \mathcal{O}(0.1)$ eV while the Yukawa couplings Y_Δ can be large. For the normally hierarchical light neutrino masses neutrino data implies very small Δ decay branching fractions to electrons and $BR(\Delta^{++} \to \mu^+\mu^+) \approx BR(\Delta^{++} \to \tau^+\tau^+) \approx BR(\Delta^{++} \to \mu^+\tau^+) \approx 1/3$. We remind also that v_Δ contributes to the SM oblique corrections, and the precision data fit $\hat{T} < 2 \cdot 10^{-4}$ [663] sets an upper bound $v_\Delta \leq 1.2$ GeV on that parameter.

At LHC Δ^{++} can be produced singly and in pairs. The cross section of the single Δ^{++} production via the WW fusion process [664] $qq \to q'q'\Delta^{++}$ scales as $\sim v^2_\Delta$. In the context of the littlest Higgs model this process, followed by the decays $\Delta^{++} \to W^+W^+$, was studied in ref. [90, 665, 666]. The detailed ATLAS simulation of this channel shows [666] that in order to observe 1 TeV Δ^{++}, one must have $v_\Delta > 29$ GeV. This is in conflict with the precision physics bound $v_\Delta \leq 1.2$ GeV as well as with the neutrino data. Therefore the WW fusion channel is not experimentally promising for the discovery of very heavy doubly charged Higgs.

On the other hand, the Drell-Yan pair production process [664, 667] $pp \to \Delta^{++}\Delta^{--}$ is not suppressed by any small coupling and its cross section is known up to next to leading order [668] (possible additional contributions from new physics such as Z' are strongly suppressed for any practical purposes). Followed by the lepton number violating decays $\Delta^{\pm\pm} \to \ell^\pm\ell^\pm$, this process allows to reconstruct $\Delta^{\pm\pm}$ invariant mass from the same charged leptons rendering the SM background to be very small in the signal region. If one also assumes that neutrino masses come from the triplet Higgs interactions, one fixes the $\Delta^{\pm\pm}$ leptonic branching ratios. This allows to test neutrino mass models at LHC.

12.2.1 Search for the final state with four muons

12.2.1.1 Introduction

The doubly charged Higgs bosons $\Delta^{\pm\pm}$ pair-produced via the Drell-Yan process is investigated assuming a branching ratio of 100% into muons. This provides an almost background free channel.

12.2.1.2 Event generation

The signal events are generated using PYTHIA, with doubly charged Higgs bosons pair-produced through the Drell-Yan process. The Higgs bosons are forced to decay into muons. Datasets are produced for several values of the doubly charged Higgs boson mass, ranging from 100 to 800 GeV/c^2.

The leading order (LO) and the next-to-leading order (NLO) cross-sections [668] are shown for the signal as a function of the doubly charged Higgs boson mass in Figure 12.4.

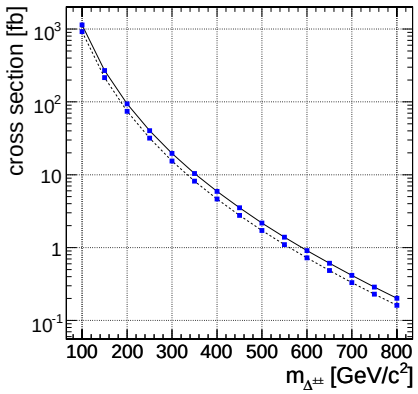

Figure 12.4: The leading order (LO) and the next-to-leading order (NLO) cross-section, for $H^{++}H^{--} \rightarrow 4\mu$.

Important backgrounds for this channel with a four muon final state are:

- $t\bar{t} \rightarrow W^+W^-b\bar{b} \rightarrow 2\mu + 2\mu$ (generated with PYTHIA).
- $Zb\bar{b} \rightarrow 2\mu + 2\mu$ (generated with COMPHEP)
- $ZZ \rightarrow 2\mu + 2\mu$ (generated with COMPHEP)
- $ZZ \rightarrow 2\tau + 2\mu$ (generated with COMPHEP)

The ZZ production process includes γ^*. The contribution of background from $b\bar{b}$ production has also been investigated. The $b\bar{b}$ background is the QCD multi-jet background which yields the highest probability to fake events with multiple muons. It has been found that the $b\bar{b}$ background can be neglected after the online selection and a cut which requires four well-reconstructed muons with pseudorapidity $|\eta| < 2.1$ and transverse momentum $p_T > 8$ GeV/c. The W bosons in the $t\bar{t}$ data sample are forced to decay into electrons, muons and taus. The tau leptons are forced to decay into electrons and muons. The Z boson in the $Z\bar{b}b$ sample is generated with $m_{Z/\gamma*} > 5$ GeV/c^2 and is forced to decay into muons. The Z bosons in the ZZ samples are forced to decay into muons and the taus in the $ZZ \rightarrow 2\tau + 2\mu$ sample decay freely.

On all samples pre-selection cuts are applied at the generation level with the following requirements:

- Final state contains two positive and two negative muons
- Transverse momentum $p_T(\mu) > 3GeVc$ and pseudorapidity $|\eta(\mu)| < 2.4$ for all muons

12.2.1.3 Event selection and reconstruction

The events are selected by dimuon trigger at Level 1 and the HLT. The p_T threshold for the dimuon HLT is 7 GeV/c. The Level 1 and HLT efficiency for the signal is $> 99\%$ within uncertainties.

The muons are reconstructed by the Global Muon Reconstructor. At least 4 muons, with a $p_T > 8$ GeV/c and $\eta \leq 2.1$, are required. The invariant mass of the doubly charged Higgs is reconstructed, by calculating the invariant mass of the two same charge muons with the highest p_T, after all cuts.

An event, where two or three muons are generated in one collision, and one or two in another, has also to be considered as background to our four muon signal. To suppress this background a vertex cut has been applied. For each muon in an event the impact point is determined. The impact point is the point of closest approach of the extrapolated muon trajectory to the nominal interaction point. The longitudinal distances Δz_{IPS} between the impact point states of all muons in one event are calculated. The biggest calculated Δz_{IPS} is required to be smaller than 0.05 cm. This is much smaller than the longitudinal size of the luminous region of the LHC beam of about 5 cm. So this cut rejects events with muons from different collision vertices with a probability of roughly 99%.

12.2.1.4 Results

Table 12.1 and Table 12.2 show the NLO production cross-section without any forced decay, the cross-section times branching ratio times pre-selection efficiency and the cross-section times branching ratio times efficiency after each stage of the online and offline event selection. Table 12.1 shows these values for each of the background samples. Table 12.2 show these values for signal samples with doubly charged Higgs masses 300, 600 and 800 GeV/c^2.

Table 12.1: The NLO cross sections σ for background events with forced decay modes after each stage of the event selection. Errors are statistical only.

	$t\bar{t}$	Zbb	$ZZ \to 4\mu$	$ZZ \to 2\mu 2\tau$
Pre-selection [fb]	232	289.8	87.4	1.63
Level-1 Trigger [fb]	232 ± 1	289 ± 1	87.3 ± 0.3	1.63 ± 0.02
High Level Trigger [fb]	149 ± 1	195 ± 1	69.7 ± 0.3	1.10 ± 0.01
4 μ reconstructed ($p_T > 8$ GeV/c, $\|\eta\| < 2.1$) [fb]	45.1 ± 0.4	25.1 ± 0.3	18.5 ± 0.1	0.25 ± 0.01
Impact Point Cut [fb]	22.8 ± 0.3	13.1 ± 0.2	16.9 ± 0.1	0.22 ± 0.01

Figure 12.5 shows the invariant mass spectrum of the reconstructed $\Delta^{\pm\pm}$ before and after the offline cuts, for $m(\Delta^{\pm\pm})$=300 GeV/c^2 and for $m(\Delta^{\pm\pm})$= 600 GeV/c^2.

12.2.1.5 Statistical interpretation

To interpret the results, the CL_s method [508] is applied, which is based on log-likelihood ratios, calculated for all bins of the invariant mass distribution. CL_s is defined as ratio of the

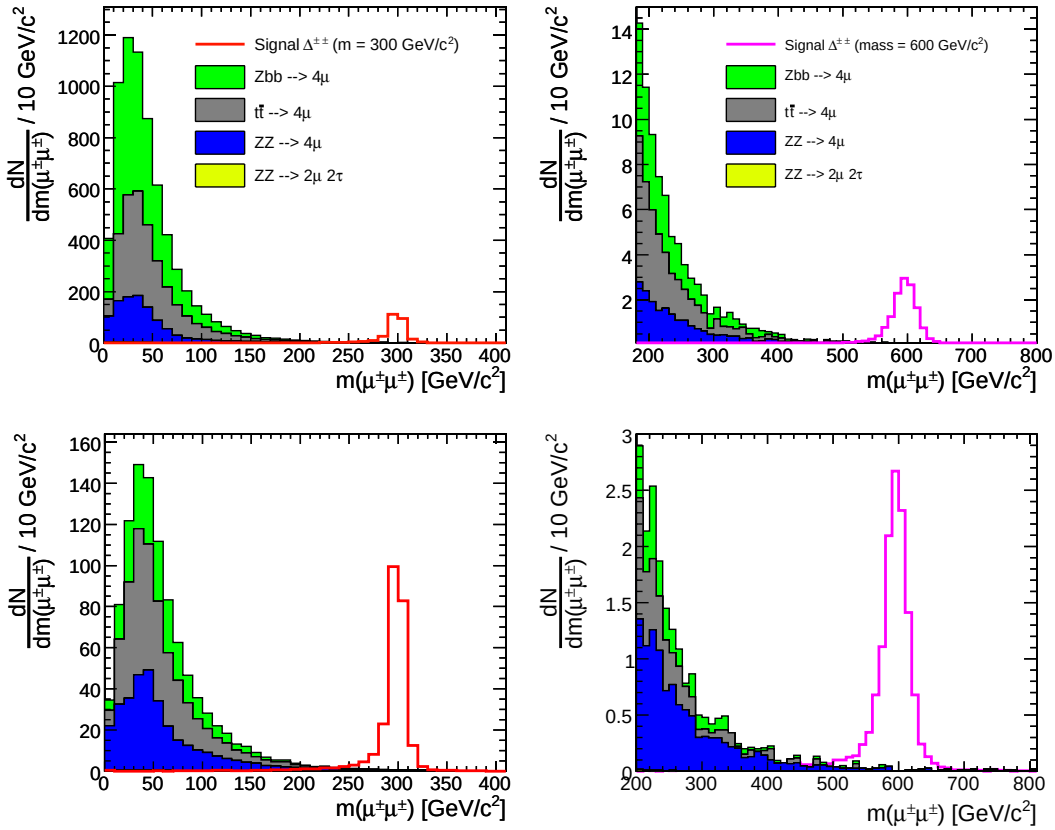

Figure 12.5: The reconstructed $\Delta^{\pm\pm}$ invariant mass after pre-selection and trigger selection (top) and after offline cuts (bottom).

Table 12.2: Production cross sections (NLO) for signal events with $m_{H^{++}} = 300$, 600, 800 GeV/c^2 and forced decay into four muons after each stage of the event selection. Errors are statistical only.

$\Delta^{\pm\pm}$ mass	300 GeV/c^2	600 GeV/c^2	800 GeV/c^2
Production cross section(NLO) [fb]	19.6	0.909	0.201
Pre-selection [fb]	17.4± 0.3	0.85 ± 0.02	0.190 ± 0.004
Level-1 Trigger [fb]	17.3 ± 0.3	0.85 ± 0.02	0.190 ± 0.004
High Level Trigger [fb]	17.1 ± 0.3	0.83 ± 0.02	0.188 ± 0.004
4 μ reconstructed ($p_T > 8$ GeV/c, $\|\eta\| < 2.1$) [fb]	13.0 ± 0.2	0.70 ± 0.02	0.158 ± 0.003
Impact Point Cut [fb]	12.5 ± 0.2	0.67 ± 0.02	0.153 ± 0.003

confidence levels for the signal and background hypotheses $CL_s = CL_{s+b}/CL_b$. CL_s can be understood as the probability of excluding an existing signal. The $1-CL_b$ can be understood as the probability for the background distribution to fake a signal. For high doubly charged Higgs boson masses the amount of simulated background events goes to zero. Nevertheless, zero simulated background events do not necessarily mean zero background events in reality. To estimate the amount of background in this region, empty bins are filled for each background with upper limits to Poisson statistic. Zero background events are compatible with maximal three generated events. Therefore empty bins get filled for each background with three events times the scale factor for an integrated luminosity of 10 fb^{-1}. The left plot in figure 12.6 shows the $1 - CL_b$ values for different doubly charged Higgs boson masses.

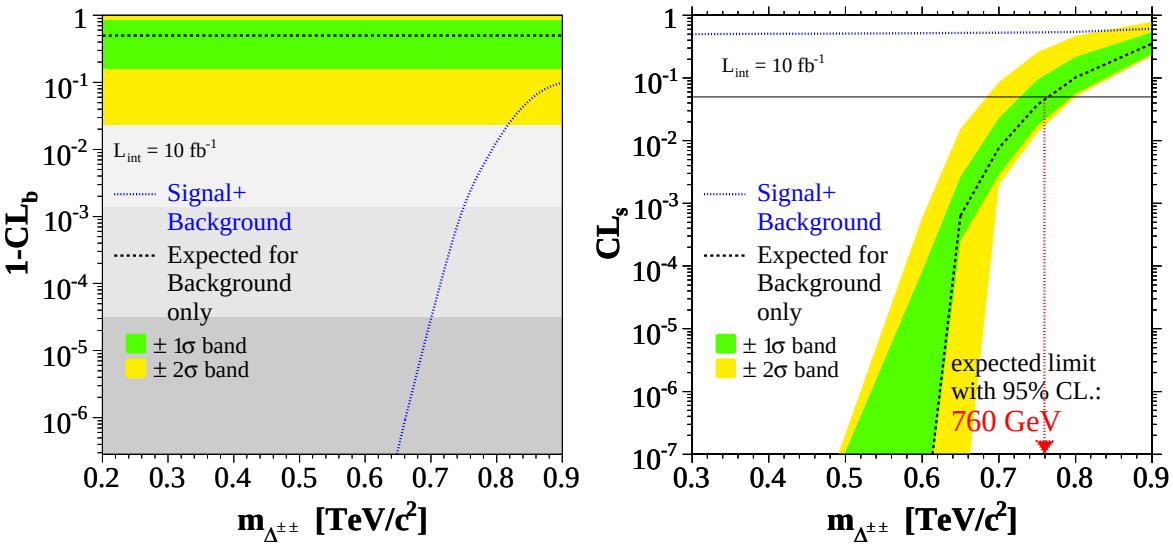

Figure 12.6: $1 - CL_b$ and CL_s as defined in the Log Likelihood Ratio Method after all selection cuts for an integrated luminosity of $10\,\text{fb}^{-1}$

For a doubly charged Higgs Boson mass smaller than $650\,\text{GeV/c}^2$ the signal plus background expectation will exceed the background only expectation by more than 5σ. To claim a discovery, at least three signal events need to be detected. For a mass of $650\,\text{GeV/c}^2$ four detectable events remain after all cuts. The right plot in figure 12.6 shows the CL_s values for different doubly charged Higgs boson masses. If no signal can be detected for an integrated luminosity of $10\,\text{fb}^{-1}$ the existence of a doubly charged Higgs Boson in this decay channel can be excluded with 95% confidence up to a mass of $760\,\text{GeV/c}^2$. The ± 1 and ± 2 -sigma bands in figure 12.6 are only for statistical errors.

12.2.1.6 Systematical uncertainties

The uncertainties on the exclusion limit resulting from systematical errors have yet to be studied in detail, once the detector is running.

The considered backgrounds are also backgrounds to the Standard Model $H \rightarrow ZZ \rightarrow 4\mu$ process. As this process is one of the benchmark processes of the future CMS detector, this backgrounds are studied in detail. The obtained total uncertainty on the background cross section is 1% to 6%. The uncertainty on signal cross section is 10% to 15%. The uncertainty on the luminosity $\mathcal{L}$ is $\sim 5\%$ for an integrated luminosity of $10\,\text{fb}^{-1}$.

Using a background cross section uncertainty of 6%, a signal cross section uncertainty of 10% and a luminosity uncertainty of 5% the approximated uncertainties on the exclusion mass limit and on the discovery mass limit are:

$$\text{Exclusion Limit} = (760\ ^{+0.5}_{-2}(\text{bkg}) \pm 10(\text{signal}) \pm 4(\text{lumi}))\,\text{GeV/c}^2 \tag{12.3}$$

$$\text{Discovery Limit} = (650\ ^{+0.4}_{-0.3}(\text{bkg})\ ^{+3}_{-0.4}(\text{signal}) \pm 0.2(\text{lumi}))\,\text{GeV/c}^2 \tag{12.4}$$

12.2.2 Search for the final states with τ leptons

12.2.2.1 Introduction

In this section we discuss the doubly charged Higgs boson pair-production via Drell-Yan process and investigate decays which involve taus and muons. The branching ratios are assumed to be $1/3$ for the following three channels: $\Delta^{\pm\pm} \to 2\mu^{\pm}$, $\Delta^{\pm\pm} \to \mu^{\pm}\tau^{\pm}$and $\Delta^{\pm\pm} \to 2\tau^{\pm}$. The reasoning comes from recent neutrino mixing measurements. As the neutrino mixing matrix and doubly charged Higgs boson decays are directly related then the appropriate branchings can be determined.

12.2.2.2 Event generation

The doubly charged Higgs boson pair-production via Drell-Yan process is generated using PYTHIA. Datasets are produced with Higgs boson mass from 200 GeV/c^2 to 600 GeV/c^2. The taus from Higgs boson decays can decay both leptonically and hadronically while in analysis we only consider hadronic decays.

The backgrounds which were considered for this analysis are as follows:

- $t\bar{t} \to \mathrm{W^+W^-}b\bar{b}$ generated by PYTHIA, COMPHEP, ALPGEN, TOPREX and MADGRAPH with W boson decay $\mathrm{W} \to \ell\nu$ ($\ell = \mathrm{e}, \mu, \tau$) forced.
- $t\bar{t}$ Z$\to W^+W^-Zb\bar{b}$ generated with COMPHEP. The W and Z bosons are allowed to decay arbitrarily.
- $\mathrm{Zb\bar{b}}$ where the Z boson decays to muons and τ leptons, generated with COMPHEP.
- ZZ generated with PYTHIA, where the Z bosons are forced to decay leptonically (e, μ, τ). The contribution of γ^* is included with m_{γ^*} >12 GeV/c^2.

The next-to-leading order (NLO) cross sections times branching ratios used for the backgrounds can be found in Table 12.3. The Monte Carlo statistics of the generated background exceed 30 fb^{-1} except $Zb\bar{b}$ background, where it is 8 fb^{-1}. Therefore the results will be presented for an integrated luminosity of 10 fb^{-1}.

Table 12.3: The NLO background processes cross sections used (in fb)

background	$t\bar{t}$ →4l	$Zb\bar{b}$	ZZ	$t\bar{t}$ Z
Cross section times BR	$88.4 \cdot 10^3$	$52.4 \cdot 10^3$	229.5	650

12.2.2.3 Event selection and reconstruction

The events are triggered by the single muon trigger at Level 1 and HLT. After HLT the event is only used if it is possible to reconstruct the event primary vertex. If the primary vertex fails to be reconstructed the event is rejected.

The muons are reconstructed using Global Muon Reconstructor. The τ leptons are reconstructed using τ-jet candidates and missing transverse energy after selection cuts. The doubly charged Higgs boson invariant mass is reconstructed from the same charge lepton pairs after all selection cuts.

The selection cuts used on muons:

- the transverse momentum must be higher than 50 GeV/c. For background events

80% of muons have $\mathrm{p_T}$ less than 50 GeV/c while for the signal with Higgs boson mass 200 GeV/c^2 it is 27% and for higher masses it reduces to around 10%.

- the distance to primary vertex in z-direction must not exceed 0.03 cm. It does not cut away any muons from the signal events but limits analysis to leptons coming from the same primary vertex.

The selection cuts used on τ jets:

- for τ jets we consider τ decays which involve 1 or 3 charged tracks. We use τ-jet candidates which passed the τ-jet filtering algorithms described in [279]. Two isolation criteria are used. Either one or three charged tracks in the signal cone and no charged tracks in the isolation cone or two tracks in signal cone and exactly one charged track in the isolation cone.
- the maximal distance to the primary vertex in the z-direction of any charged track in the τ jet must not exceed 0.2 cm.
- the transverse energy of the hottest HCAL tower of the τ jet must be higher than 2 GeV. This cut eliminates 86% of all electrons taken as τ candidates and only removes 7.5% of real τ jets.
- the transverse energy of the τ jet candidate must exceed 50 GeV. It has been chosen to be the same as the cut used on muons.
- no muon track should be in a cone with $\Delta R = 0.3$ constructed around the τ-jet candidate. If there is, then the candidate is dropped. This eliminates false τ-jet candidates which are generated when a charged muon track passes the same region as photons or hadrons. With this cut only a few real τ jets are discarded however most of the false τ jets coming from this misidentification are rejected.

Missing transverse energy ($E_{\mathrm{T}}^{\mathrm{miss}}$) is reconstructed using calorimeter Type 1 $E_{\mathrm{T}}^{\mathrm{miss}}$ ($E_{\mathrm{T}}^{\mathrm{miss}}$ with the jet energy corrections) and $\mathrm{p_T}$ of muons.

Only events with at least four objects, muons or τ jets, are accepted. The possible final states are:

- $\Delta^{++}\Delta^{--} \to 4\mu$ - this channel is investigated in the previous subsection.
- $\Delta^{++}\Delta^{--} \to 3\mu 1\tau$ - this channel is easily reconstructible as there is only one neutrino and it goes the direction of the τ jet.
- $\Delta^{++}\Delta^{--} \to 2\mu 2\tau$ - this channel can also be reconstructed using the assumption that the neutrinos go in the same directions as the τ jets.
- $\Delta^{++}\Delta^{--} \to 1\mu 3\tau$ - this channel can be reconstructed only with very good $E_{\mathrm{T}}^{\mathrm{miss}}$ resolution as it requires an additional assumption that the masses of the two reconstructed Higgs bosons are the same. However the reconstruction is very sensitive to $E_{\mathrm{T}}^{\mathrm{miss}}$ accuracy and often the event has to be dropped due to negative τ-lepton energies.
- $\Delta^{++}\Delta^{--} \to 4\tau$ - this channel can not be reconstructed (and triggered by the single muon trigger).

Once the event leptons are reconstructed, some additional selections are performed:

- Z boson veto - if the odd sign pairing gives an invariant mass of 91 ± 5 GeV/c^2 then these leptons are removed from further use.

- Same charge lepton pairs are reconstructed and only those reconstructed Higgs candidate pairs whose invariant mass difference is within 20% of each other are considered.

The reconstructed mass of doubly charged Higgs boson is shown on Figures 12.7 for the Higgs boson masses 200 and 500 GeV/c^2.

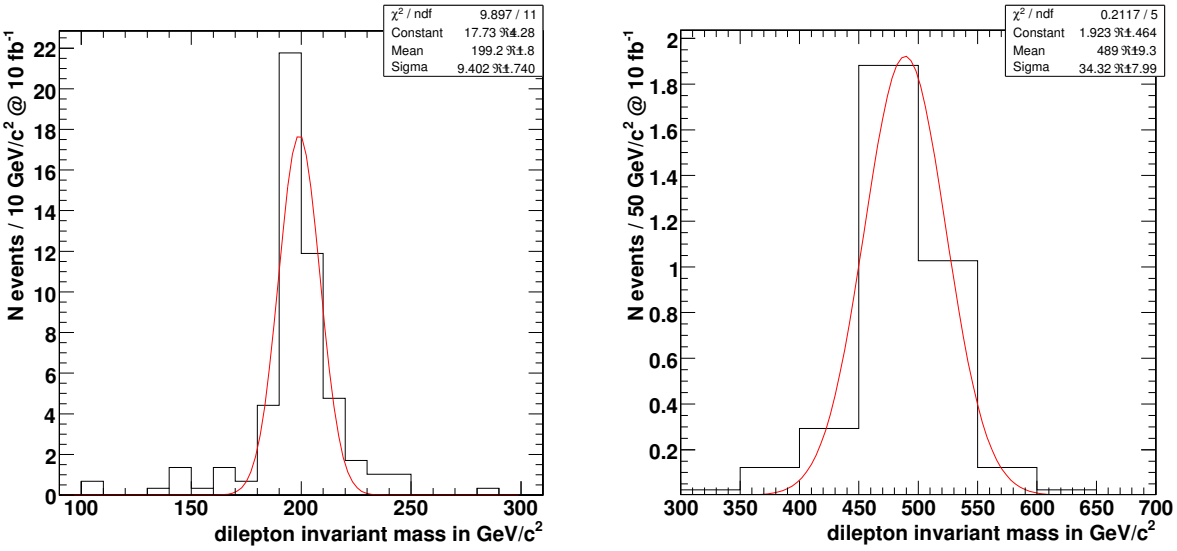

Figure 12.7: The reconstructed invariant mass for M($\Delta^{\pm\pm}$)=200 GeV/c^2 and 500 GeV/c^2.

12.2.2.4 Selection efficiencies

The upper limit of the signal selection efficiency is given by the fraction of events with $3\mu1\tau$, $2\mu2\tau$, $1\mu3\tau$ ($\tau \rightarrow$ hadrons) topology relative to all possible final states with muons and τ leptons from decays of two Higgs bosons. Assuming the above mentioned branching ratios the upper limit is $\simeq 35\%$. The fraction of every selected topology is given below:

- $\Delta^{++}\Delta^{--} \rightarrow 3\mu1\tau = 2/9 \text{ events} \times 0.65 = 14.4\%$.
- $\Delta^{++}\Delta^{--} \rightarrow 2\mu2\tau = 3/9 \text{ events} \times 0.65^2 = 14.1\%$.
- $\Delta^{++}\Delta^{--} \rightarrow 1\mu3\tau = 2/9 \text{ events} \times 0.65^3 = 6.1\%$.

where 0.65 is the branching ratio of $\tau \rightarrow$ hadrons decays. Table 12.7 summarises the efficiencies of each selection (relative to the previous one) for the signal of different $\Delta^{\pm\pm}$ masses. The lepton selection efficiency and purity is shown in Table 12.5. Background efficiencies are shown in Table 12.6.

Table 12.4: The signal selection efficiencies for different $\Delta^{\pm\pm}$ masses. Total efficiency is the product of the single efficiencies.

$m_{\Delta}^{\pm\pm}$ (GeV/c^2)	200	300	400	500	600
Level 1 and HLT	83.7%	86.0%	86.7%	85.8%	88.3%
Primary vertex	96.9%	98.5%	97.0%	97.5%	98.0%
4 leptons in final state	10.1%	17.2 %	23.6%	24.7%	26.7%
two pairs and at least one τ	44.9%	46.1%	41.7%	53.2%	52.9%
Mass difference	62.5%	77.2%	80.4%	74.3%	63.6%
Total signal efficiency	2.3%	5.1%	6.6%	8.1%	7.7%

Table 12.5: Single muon and τ selection efficiencies and purity.

$m_{\Delta}^{\pm\pm}$ (GeV/c^2)	200	300	400	500	600
Single μ selection efficiency	70.7%	82.0%	86.1%	87.2%	89.2%
1 - purity of accepted muons:	0.1%	0.4%	0.8%	0.7%	1.0%
Single τ selection efficiency	36.6%	42.3%	50.6%	53.3%	53.3%
1 - purity of accepted τ jets:	2.2%	2.2%	4.2%	3.6%	3.2%

Table 12.6: Selection efficiencies for background. Total efficiency is the product of the single efficiencies.

Process	$t\bar{t}$	$t\bar{t}$ Z	ZZ	Zbb
Level 1 and HLT trigger	40.7%	20.3%	40.0%	42.1%
Primary vertex	99.3%	99.8%	96.7%	98.2%
4 leptons in final state	0.0015%	0.04 %	3.0%	0.0005%
two pairs and at least one τ	-	0.1%	-	-
Mass difference	-	100%	-	-
Total signal efficiency	-	0.0008%	-	-

12.2.2.5 Systematic errors

At the integrated luminosity of 10 fb^{-1} the cuts implemented above result in an almost background free signal. For datasets with Monte Carlo statistics above 30 fb^{-1} giving zero Monte Carlo events after all selections ($t\bar{t}$, ZZ^*) we assume the background to be zero. For $t\bar{t}Z$ background where is one Monte Carlo event passing all cuts, which corresponds to 0.05 expected events when scaled with cross section and luminosity. For $Zb\bar{b}$ background where the Monte Carlo statistics corresponds to 8 fb^{-1} no events passed all cuts. The analysis was repeated with p_{T} cut on muon (τ jet) of 40 GeV/c, 30 GeV/c and 20 GeV/c, again with no events passing the cuts, which confirms the assumption that leptons coming from $Zb\bar{b}$ are too soft to produce a background. Considering the smallness of all backgrounds we assume no background at 10 fb^{-1} for the following analysis.

The systematic uncertainties used for the signal are the following:

- muon misidentification ($\Delta\mu$) - 1% per muon.
- muon isolation ($\Delta\mu_{isol}$)- 2% per event.
- τ jets identification ($\Delta\tau$)- 9% per τ jet.
- luminosity ($\Delta\mathcal{L}$) - 5%.
- PDF and scale ($\Delta\sigma$)- 10% (theoretical uncertainty, it is not used for the signal cross section measurement with no background).

As the events are a mixture of different decay modes the total selection efficiency uncertainty ($\Delta\varepsilon_S$) is calculated per decay channel and then added together with the corresponding weights:

$$\Delta 3\mu 1\tau = \sqrt{3\Delta\mu^2 + \Delta\tau^2} = 8.2\%,$$

$$\Delta 2\mu 2\tau = \sqrt{2\Delta\mu^2 + 2\Delta\tau^2} = 11.4\%,$$

$$\Delta 1\mu 3\tau = \sqrt{\Delta\mu^2 + 3\Delta\tau^2} = 13.9\%,$$

giving

$$\Delta\varepsilon_S = \frac{144\Delta 3\mu 1\tau + 141\Delta 2\mu 2\tau + 61\Delta 1\mu 3\tau}{346} = 10.5\%$$

The total systematic error for cross section measurement is then

$$\frac{\Delta\sigma}{\sigma} = \sqrt{\Delta\mu_{isol}{}^2 + \Delta\mathcal{L}^2 + \Delta\varepsilon_S{}^2} = 13\%.$$

The statistical errors were evaluated constructing the shortest Bayesian confidence interval for the confidence level of 67 % [669].

12.2.2.6 Results

The expected number of events at 10 fb^{-1} and the NLO cross section with expected statistical and systematic uncertainty of the cross section measurement are given in Table 12.7. Table 12.7 shows also the integrated luminosity needed for exclusion at 95% CL.

Table 12.7: Expected number of events, NLO cross section with expected statistical and systematic uncertainty of the cross section measurement at 10 fb^{-1}, and integrated luminosity needed for exclusion at 95% CL.

$m_\Delta^{\pm\pm}$ (GeV)	200	300	400	500
N_{ev} expected at 10 fb^{-1}	26	10	4	2
$\sigma_{\rm NLO} \pm {\rm stat} \pm {\rm syst}$ (fb)	$93.9^{+19.3}_{-17.5} \pm 12.2$	$19.6^{+6.6}_{-5.6} \pm 2.5$	$5.9^{+3.4}_{-2.5} \pm 0.8$	$2.2^{+1.9}_{-1.3} \pm 0.3$
Luminosity for 95% CL exclusion, fb^{-1}	1.3	3.0	7.7	16.8